Molecular Therapy
Nucleic Acids
Original Article

Comprehensive characterization of a drug-resistance-related ceRNA network across 15 anti-cancer drug categories

Bing Liu,[1,3,8] Xiaorui Zhou,[5,8] Dongyuan Wu,[6] Xuesong Zhang,[7] Xiuyun Shen,[4] Kai Mi,[2] Zhangyi Qu,[1] Yanan Jiang,[2,3,4] and Desi Shang[2]

[1]Department of Biopharmaceutical Sciences, College of Pharmacy, Harbin Medical University, Harbin 150081, P.R. China; [2]College of Bioinformatics Science and Technology, Harbin Medical University, Harbin 150081, P.R. China; [3]Translational Medicine Research and Cooperation Center of Northern China, Heilongjiang Academy of Medical Sciences, Harbin 150086, P.R. China; [4]Department of Pharmacology (State-Province Key Laboratories of Biomedicine-Pharmaceutics of China, Key Laboratory of Cardiovascular Research, Ministry of Education), College of Pharmacy, Harbin Medical University, Harbin 150081, P.R. China; [5]BGI Education Center, University of Chinese Academy of Sciences, Shenzhen 518083, P.R. China; [6]Department of Pharmacy, Harbin Medical University Cancer Hospital, Harbin 150030, P.R. China; [7]Department of Stomatology, 962 Hospital of PLA, Harbin 150080, P.R. China

Cancer is still a major health problem around the world. The treatment failure of cancer has largely been attributed to drug resistance. Competitive endogenous RNAs (ceRNAs) are involved in various biological processes and thus influence the drug sensitivity of cancers. However, a comprehensive characterization of drug-sensitivity-related ceRNAs has not yet been performed. In the present study, we constructed 15 ceRNA networks across 15 anti-cancer drug categories, involving 217 long noncoding RNAs (lncRNAs), 158 microRNAs (miRNAs), and 1,389 protein coding genes (PCGs). We found that these ceRNAs were involved in hallmark processes such as "self-sufficiency in growth signals," "insensitivity to antigrowth signals," and so on. We then identified an intersection ceRNA network (ICN) across the 15 anti-cancer drug categories. We further identified interactions between genes in the ICN and clinically actionable genes (CAGs) by analyzing the co-expressions, protein-protein interactions, and transcription factor-target gene interactions. We found that certain genes in the ICN are correlated with CAGs. Finally, we found that genes in the ICN were aberrantly expressed in tumors, and some were associated with patient survival time and cancer stage.

INTRODUCTION

Cancer is the second leading cause of death globally.[1] It is estimated that there were 18.1 million new cases of cancer and 9.6 million deaths from cancer in 2018.[2] Drug resistance refers to some types of cancers that are not sensitive to certain or multiple kinds of drugs, which is a key issue in the treatment of cancer. The emergence of resistance toward existing drugs is a major challenge in treating cancer. Most advanced-stage cancers are not sensitive to conventional therapies. Even though targeted therapies improved the clinical treatment of a certain number of difficult-to-treat cancers, their efficiencies are various depending on the different types of cancer and genetic backgrounds of patients.[3] Additionally, biomarkers for the diagnosis and prognosis of drug resistance are also urgently needed. Therefore, finding new ways to overcome the drug resistance of various cancers has drawn the attention of many researchers.

Numerous studies have been conducted to identify the molecular mechanisms of drug resistance. The effects of coding and noncoding genes in drug resistance have been widely investigated regarding the efflux of drugs, the inhibition of cell death, and then induction of epithelial-mesenchymal transition (EMT), among other factors.[4–6] In the initial stage of exploration, researchers mainly focused on the alteration of coding genes. For instance, ATM deficiency is associated with sensitivity to poly (ADP-ribose) polymerase-1 (*PARP1*) and ataxia telangiectasia mutated and Rad3 related (*ATR*) inhibitors in lung adenocarcinoma.[7] In recent decades, noncoding genes have also been reported to play important roles in drug resistance. Based on their length, noncoding genes can generally be classified as microRNAs (miRNAs or miRs) or long noncoding RNAs (lncRNAs). miRNAs mediate gene expression regulatory effects at the post-transcriptional level. For example, overexpression of miR-130b promotes adriamycin resistance in breast cancer cells by targeting *PTEN*.[8] Circulating exosomal miR-96 promotes the progression and cisplatin resistance of lung cancer by targeting *LMO7*.[9] lncRNAs are also correlated with metastasis, drug resistance, and clinical outcome in

Received 20 February 2020; accepted 9 February 2021;
https://doi.org/10.1016/j.omtn.2021.02.011.

[8]These authors contributed equally

Correspondence: Desi Shang, College of Bioinformatics Science and Technology, Harbin Medical University, Harbin 150081, P.R. China.
E-mail: sds_46@163.com
Correspondence: Zhangyi Qu, Department of Biopharmaceutical Sciences, College of Pharmacy, Harbin Medical University, Harbin 150081, P.R. China.
E-mail: hmu635@126.com
Correspondence: Yanan Jiang, College of Bioinformatics Science and Technology, Harbin Medical University, Harbin 150081, P.R. China.
E-mail: jiangyanan@hrbmu.edu.cn

cancer.[10] The expression of lncRNA *HOTAIR* is upregulated in various cancers, including lung cancer, breast cancer, and pancreatic cancer, among others.[11–13] Its upregulation decreases the sensitivity of lung cancer cells to cisplatin.[14] lncRNA activated by transforming growth factor (TGF)-β (*ATB*) is highly expressed in breast cancer tissues and cells, which could predispose patients to the invasion-metastasis cascade and trastuzumab resistance.[15] The upregulation of lncRNA cancer upregulated drug resistant (*CUDR*) was observed in doxorubicin-resistant human squamous carcinoma cells. This overexpression could promote the resistance of squamous carcinoma cells to doxorubicin and etoposide.[16] Therefore, coding and noncoding genes are both closely related to the drug sensitivity of cancer cells. However, the interaction between coding and noncoding genes in drug resistance has not been fully explored.

In recent years, Salmena et al.[17] proposed a new way to reveal the interaction between noncoding and coding RNAs, that is, a competing endogenous RNA (ceRNA) theory. The roles of ceRNA triplets including lncRNAs, miRNAs, and protein coding genes (PCGs) have been confirmed in various pathological and physiological conditions, and especially in the drug sensitivity of cancers. lncRNA ARSR promotes doxorubicin and sunitinib resistance in cancers, which occurs at least partially via competitive binding of miR-34/miR-449.[18,19] The downregulation of lncRNA *GAS5* upregulates miR-222 expression, which confers tamoxifen resistance in breast cancer.[20] Current studies suggest that lncRNAs are responsible for the multi-drug resistance of cancers. Moreover, the ceRNA mechanism plays an important role in drug resistance. However, there is currently a lack of understanding concerning the global drug-sensitivity-related ceRNA networks across different drug categories.

With the development of pharmacogenomics, the collection of a large amount of drug-sensitivity-related gene profile data has facilitated the prediction of the mechanism of drug sensitivity. Therefore, large-scale ceRNA networks involving different drug categories need to be constructed, as these would be helpful in elucidating the mechanism of drug resistance and promoting the rational use of drugs. The present study aimed to construct and analyze a drug-sensitivity-related ceRNA network across 15 anti-cancer drug categories. The topological properties of the networks were investigated and an intersection ceRNA network (ICN) across 15 anti-cancer drug categories was constructed. Moreover, some genes in the ICN were found to be correlated with clinically actionable genes (CAGs) and have clinical relevance.

RESULTS

Global landscape and comparison of ceRNA networks across 15 anti-cancer drug categories

To investigate the role of ceRNA triplets (lncRNAs-miRNAs-PCGs) and the competitive patterns of drug-sensitivity-related ceRNAs, we constructed 15 ceRNA networks across 15 anti-cancer drug categories (Figure 1; Table S1). A total of 105,255 ceRNA interactions were identified, involving 217 lncRNAs, 158 miRNAs, and 1,389 PCGs. The largest ceRNA network belonged to YK (1,759 nodes and 9,334 edges), whereas the smallest ceRNA network belonged to Df (1,460 nodes and 4,661 edges). The number of lncRNAs, miRNAs and PCGs, as well as the nodes and edges of the ceRNA networks for each anti-cancer drug category, are shown in Table 1. The 15 ceRNA networks across 15 anti-cancer drug categories are shown in Figure 1. Kyoto Encyclopedia of Genes and Genomes (KEGG) pathway analyses were performed for 15 ceRNA networks (Figure S1). Some signaling pathways were shared by all drug categories, including "pathways in cancer," "microRNAs in cancer," "PI3K-Akt signaling pathway," and "cell cycle," among others, while some signaling pathways were drug type specific, involving "pertussis," "tuberculosis," "herpes simplex infection," and "Ras signaling pathway," among others. The topological evaluation of the ceRNA networks showed that the degrees of these ceRNA networks all obeyed a power law distribution, which conforms to the characteristics of biological networks (Figure S2). The node proportion of each ceRNA network is shown in Figure S3. The original data of the 15 ceRNA networks are shown in Data S1.

To explore the specificities and similarities across the 15 ceRNA networks, we compared their components of lncRNAs, miRNAs, and PCGs by calculating the Jaccard coefficients. The results showed that the ceRNA molecules, including lncRNAs and miRNAs, were more conserved in the 15 ceRNA networks, while the miRNAs tended to be shared among the different ceRNA networks (Figures 2A–2C). In contrast, PCGs displayed the lowest similarities across these drug categories (Figures 2C and 2D). The average values of the Jaccard coefficients of the lncRNAs, miRNAs, and PCGs are shown in Figure 2D. Then, we compared the distribution of lncRNAs, miRNAs, and PCGs among all ceRNA networks (Figure 2E). The results indicated that more lncRNAs and miRNAs were shared by different drug categories than PCGs.

We also compared the hub nodes in the 15 ceRNA networks. Hub nodes were identified as the highly connected nodes, which were considered to play a critical role in the maintenance of network stability.[21–24] In this study, the lncRNA and PCG nodes with the top 5% highest degree and degree >10 were defined as hub nodes.[24] A total of 98 hubs were defined across the 15 ceRNA networks. Among them, 56 hub nodes were shared by all networks. These shared hub nodes belong to lncRNAs, including *XIST*, *H19*, *TUG1*, and *NEAT1*, among others (Figure 2F). Additionally, there are also some specific hub nodes, including *CDKN1A*, *VEGFA*, *BCL2*, and *CDK6* (Figure 2F).

In addition, we examined the properties of lncRNAs in these ceRNA networks. The classes of lncRNAs in the 15 ceRNA networks were identified according to lncRNA annotation (see Materials and methods). The results showed that most of these competitive lncRNAs were classified as long intergenic noncoding RNA (lincRNA), antisense, and processed transcripts (Figure S4). lincRNAs show broad biological activity through interacting with miRNAs.[25,26] These results provided evidence that ceRNAs may be a fundamental layer of gene regulation in drug resistance. We further analyzed the ceRNA triplets and found that almost all of the lncRNAs, miRNAs, and PCGs were

Figure 1. ceRNA networks of 15 anti-cancer drugs

Circular pink nodes represent miRNAs; triangular purple nodes represent lncRNAs; square green nodes represent PCGs.

located in different chromosomes (Figure S5). This indicates that the ceRNA triplet interactions tend to be through distant regulation, which is also consistent with ceRNA theory.

Relevance between ceRNAs across 15 drug categories and cancer hallmark processes

Next, we investigated the role of these ceRNAs across 15 drug categories in cancer. To do this, we obtained cancer-related lncRNAs, miRNAs, and PCGs from several databases (see Materials and methods). The relevance between ceRNAs and cancer hallmarks was calculated using a hypergeometric test. Competing triplets that enriched lncRNAs, miRNAs, and PCGs of each drug category are shown in Figure 3A. The results indicated that miRNA, which mediates lncRNA-PCG competition pairs, is more likely to be related to cancers (Figure 3A). The hypergeometric test result of Figure 3A is shown in Table S2.

Table 1. Statistical results for the ceRNA networks across 15 anti-cancer drug categories

MOA	miRNAs	lncRNAs	PCGs	Nodes	Edges
YK	158	217	1,384	1,759	9,334
Df	149	213	1,044	1,406	4,661
Ds	157	217	1,369	1,743	8,831
A7	158	217	1,379	1,754	9,241
AM	156	216	1,329	1,701	8,103
Db	151	211	1,073	1,435	5,299
Ho	158	217	1,380	1,755	9,085
Rs	146	209	1,140	1,495	4,423
Tu	155	217	1,346	1,718	8,167
T2	154	216	1,290	1,660	7,890
Apo	151	212	1,108	1,471	6,015
DNMT	148	209	1,104	1,461	4,390
STK	150	213	1,220	1,583	5,731
T1	152	209	1,049	1,410	4,597
Pr	145	210	1,078	1,433	4,302

MOA, mechanism of action.

We then explored whether these PCGs for each drug category were targeting cancer hallmark processes.[27] After collecting the cancer hallmark processes, the Jaccard coefficient was used to measure intersections between cancer hallmark genes and PCGs in each ceRNA network. The results showed that PCGs in the ceRNA networks were represented across a broad range of cancer hallmarks (Figure 3B). The hypergeometric test result of Figure 3B is shown in Table S3. In particular, hallmarks including "self-sufficiency in growth signals" and "insensitivity to antigrowth signals" were the two most significantly enriched terms across different drugs. These findings suggest that these cancer hallmarks tend to be common among different drugs and also further confirm the existence of a common network of anti-cancer drug-sensitivity-related ceRNAs. A number of genes were correlated with multi-drug resistance.

Construction of the ICN across the 15 ceRNA networks and analysis of its therapeutic potential

We found that there are many intersections of lncRNAs, miRNAs, and PCGs among the 15 ceRNA networks (Figures 2 and 3). This raises the question of whether intersections exist among the ceRNA networks across the 15 drug categories. And, if they do, what are their functions?

To determine this, we extracted the intersection edges of the 15 ceRNA networks and constructed an ICN, which is composed of 7 lncRNAs, 13 miRNAs, and 32 PCGs (Figure 4). This showed that *H19* is the most connected lncRNA node in the ICN, which may regulate key signaling pathways in drug resistance (Figure 4). Some of the predicted relationships have been verified using HT29 and methotrexate-resistant HT29 (HT29-MTX) colon cancer cell lines. Compared with HT29 cells, the expression of *HIF1A* and *H19* was upregulated in HT29-MTX cells (Figures S6A and S6B). Additionally, the knockdown of *H19* upregulated miR-20a-5p, miR-20b-5p, and miR-17-5p in HT29-MTX cells (Figures S6C–S6F). Also, to validate the ceRNA network of lncRNA H19/miRNA/HIF1A, an additional experiment was conducted. A dual-luciferase reporter assay was used to validate the direct interaction between miR-17-5p and H19/HIF1A. The results showed that miR-17-5p could directly bind to *H19* and *HIF1A*. Additionally, the knockdown of *H19* could upregulate miR-17-5p and downregulated *HIF1A* mRNA and protein (HIF-1α) expression levels, which was attenuated by miR-17-5p inhibition (Figure S7).

To show the effect of the ICN on drug response, we analyzed the correlation between drug sensitivity to 76 US Food and Drug Administration (FDA)-approved anti-cancer drugs and the transcriptional expression of genes in the ICN (Figure 5). The correlation between the expression of genes in the ICN and drug sensitivity is shown in Figure S8.

Interaction between CAGs and genes in the ICN

To further understand the clinical implications of the ICN, the expression profiles of genes in the ICN were correlated with CAGs. CAGs are FDA-approved drug target genes and associated biomarker genes, including 132 target therapeutic genes and 19 immunotherapeutic genes. The expression profiles of 151 genes were obtained and Pearson's correlation coefficient (PCC) values were calculated (Figure 6). Gene pairs with PCCs $|R| > 0.3$ and a false discovery rate (FDR) < 0.05 were screened. We observed that 94.7% of the CAGs were associated with genes in the ICN (Figure 6). Genes in the ICN were also correlated with CAGs. Among them, some protein-protein interactions (PPIs) and transcriptional factor-gene interactions were observed (Figure 6). These results showed that CAGs could be regulated by ceRNAs, including through targeted therapy and immunotherapy. This data analysis was based on the PPI and transcription factor (TF) data from the Human Protein Reference Database (HPRD) (http://www.hprd.org/)[28] and BioGRID (https://thebiogrid.org/) databases.[29] The results showed that ceRNAs have many effects on CAGs. Therefore, the significant interactions between CAGs and ceRNA-associated genes may affect the drug response.

Clinical relevance of the ICN

We then explored the association of genes in the ICN with patient survival time and cancer stage. We identified 1 lncRNA, 13 miRNAs, and 33 PCGs associated with overall survival in at least one cancer type (Figure 7A). Most of the genes in the ICN were negatively correlated with the survival of brain low-grade glioma (LGG) patients, while only a small number of these genes showed a correlation with that of acute myeloid leukemia (LAML) patients. Also, many genes in the ICN were correlated with patient survival time and cancer stage of kidney renal clear cell carcinoma (KIRC), stomach adenocarcinoma (STAD), and breast invasive carcinoma (BRCA). Some genes act as either promotors or suppressors of cancers and are closely

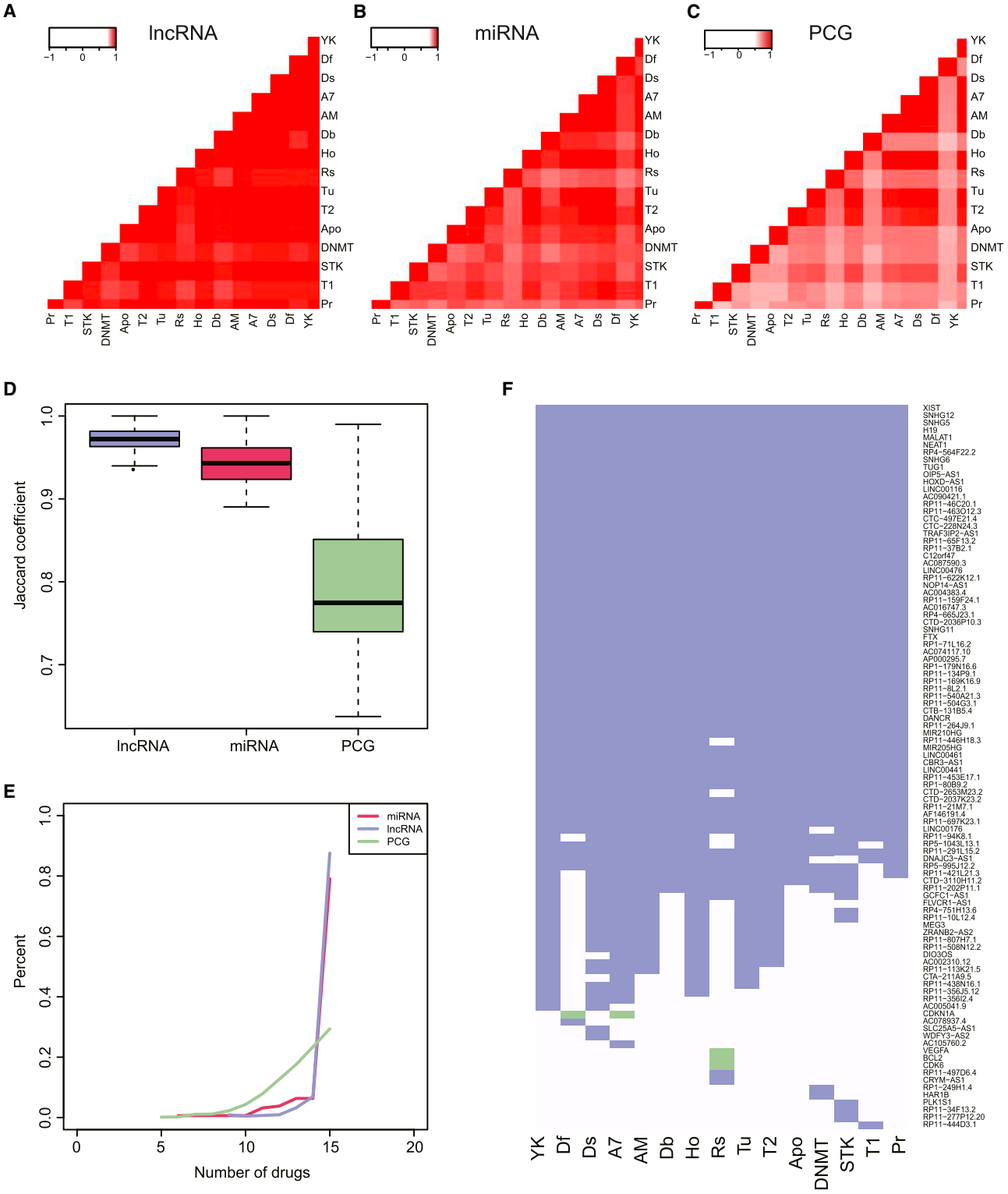

(legend on next page)

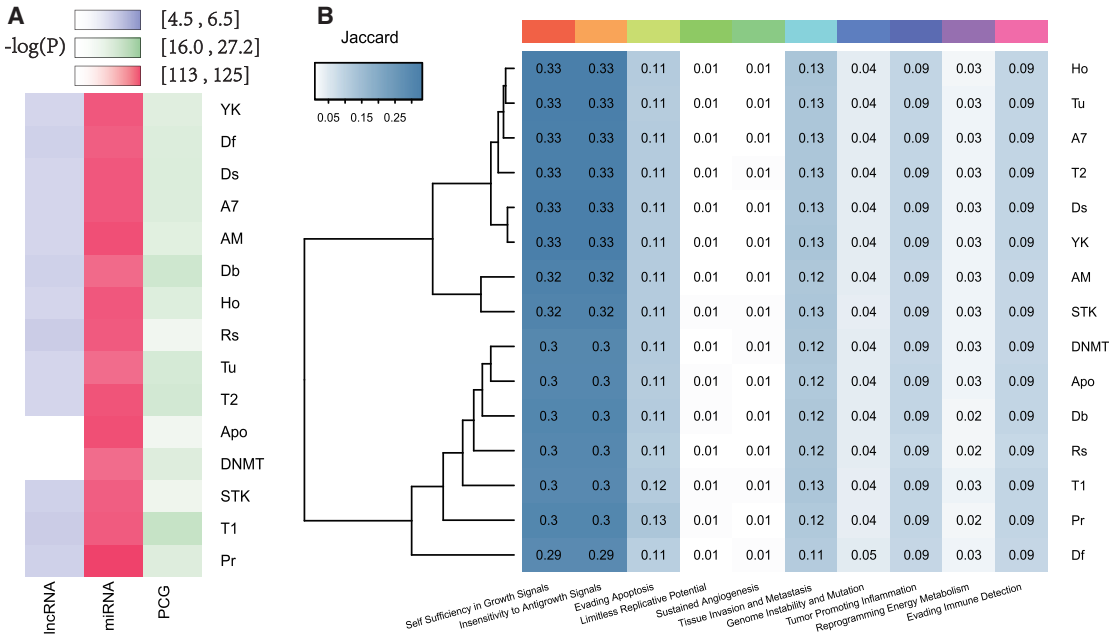

Figure 3. Relevance between ceRNAs across the 15 drug categories and cancer hallmark processes

(A) p values of the hypergeometric test that evaluated the significance of overlap between 15 ceRNA networks and cancer-lncRNAs, miRNAs, and PCGs, respectively. (B) Jaccard coefficient matrix for PCGs in the pan-drug ceRNA networks and cancer hallmark processes.

correlated with the outcome of patients. For example, patients with a low expression level of *E2F2* showed significantly worse survival in head and neck squamous cell carcinoma (HNSC) (log-rank test, p = 0.0018), STAD (log-rank test, p = 0.018), and rectum adenocarcinoma (READ) (log-rank test, p = 0.018) (Figure 7B). In contrast, several other genes promote the progression of cancer. *ITGB8* is taken as an example. The enhanced expression of *ITGB8* was associated with worse survival in bladder urothelial carcinoma (BLCA) (log-rank test, p = 0.021), LGG (log-rank test, p < 0.0001), and pancreatic adenocarcinoma (PAAD) (log-rank test, p = 0.0023) patients (Figure 7B).

DISCUSSION

Drug resistance continues to be a major factor in treatment failure of cancers. In recent years, the ceRNA has become a research hotspot, as it reveals a new way to regulate gene expression. A large number of studies have shown that ceRNAs play important roles in the pathogenesis and treatment of cancer. A recent study revealed the role of ceRNA modules in drug resistance across multiple cancers through ceRNA network-based drug sensitivity prediction.[30] In the present study, we systematically constructed and dissected ceRNA networks across 15 anti-cancer drug categories.

Fifteen ceRNA networks were constructed across 15 anti-cancer drug categories. The largest ceRNA network belongs to YK, which represents tyrosine kinase inhibitor. Although YK therapy is widely used clinically, there may also exist a small population of insensitive cancer cells that lead to treatment failure, manifesting as minimal residual disease.[31] Consistent with this, we found the ceRNA network based on YK has the largest number of shared hub nodes. There are also some specific hub nodes shown in Figure 2F, including *CDKN1A*, *VEGFA*, *BCL2*, and *CDK6*. Among them, *CDKN1A* is the specific hub node of both Df and A7 drug categories. Rs has the largest number of specific hub nodes, involving *EGFA*, *BCL2*, and *CDK6*. These genes are potential drug sensitivity markers. Therefore, the identification of these specific hub nodes may promote personalized treatment in the clinic.

Across the 15 ceRNA networks, we found that hub nodes tend to be shared by various ceRNA networks. Of all the hub nodes identified across the 15 ceRNA networks, 56 of them are shared by all networks. The hub nodes belonging to lncRNAs include *XIST*, *H19*, *TUG1*, *NEAT1*, and others. These hub genes have been shown to be related to drug resistance. lncRNA *XIST* is downregulated in recurrent cancer, and its expression level correlates significantly with Taxol

Figure 2. Similarities across the 15 ceRNA networks and hub nodes analysis

(A) Correlation of lncRNAs across the 15 ceRNA networks. (B) Correlation of miRNAs across the 15 ceRNA networks. (C) Correlation of PCGs across the 15 ceRNA networks. (D) Average values of the Jaccard coefficients of lncRNAs, miRNAs, and protein coding genes (PCGs). (E) Distribution map of the number of drug types in the 15 ceRNA networks. (F) Hub analysis of the ceRNA networks across the 15 anti-cancer drug categories. Distribution of the hub genes across the pan-drug ceRNA networks is shown. Purple boxes represent lncRNAs and green boxes represent PCGs.

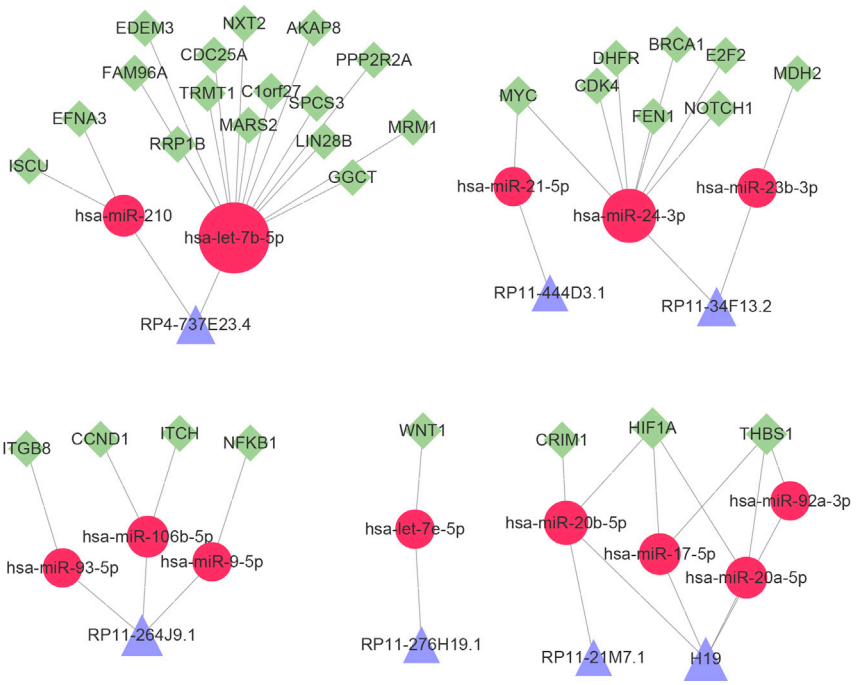

Figure 4. Intersection ceRNA networks (ICNs) of different drugs

Circular pink nodes represent miRNAs; triangular purple nodes represent lncRNAs; and square green nodes represent PCGs.

(paclitaxel) sensitivity in ovarian cancer.[9] In contrast, it was upregulated in doxorubicin-resistant colorectal cancer tissues and cells. The interference of lncRNA *XIST* enhanced the anti-cancer effect of doxorubicin in colorectal cancer through the regulation of the miR-124/SGK1 axis.[32] lncRNA *NEAT1* could act as a ceRNA to upregulate epigallocatechin-3-gallate (EGCG)-induced CTR1 by sponging hsa-miR-98-5p, thus enhancing the cisplatin sensitivity of non-small cell lung cancer (NSCLC) cells.[33] lncRNA *H19* is upregulated in cisplatin- and methotrexate-resistant cancer cells. The expression of *H19* was negatively correlated with the cisplatin-based chemotherapy response in ovarian cancer patients.[34] Knockdown of *H19* promoted the sensitivity of colorectal cancer to methotrexate.[11] These findings indicate that hub nodes may play important roles in drug resistance.

We investigated the relevance of ceRNAs across 15 drug categories and cancer hallmark processes. The results showed that ceRNAs were enriched in the cancer genes. This indicates that genes in the ceRNA networks are highly conserved and are also crucially relevant in various cancers. Compared with lncRNAs and PCGs, miRNAs were more likely to be associated with cancers. Cancer hallmark functional analysis revealed that these ceRNAs were related to hallmark processes such as "self-sufficiency in growth signals," "insensitivity to antigrowth signals," and "tissue invasion and metastasis" (Figure 3). These functions are all drug resistance-associated biological processes in cancer cells.

We then explored the specificities and similarities among the 15 ceRNA networks. Interestingly, although these drug categories have dramatically different molecular mechanisms, they shared many ceRNAs. Additionally, the constructed 15 ceRNA networks across 15 drug categories had many intersections. These findings suggested that there may be an intersection ceRNA network across different anti-cancer drug categories. Therefore, we speculated that there exists a common ceRNA network across the 15 drug categories. An ICN was constructed as expected (Figure 4). lncRNA *H19* is the hub node across 15 ceRNA networks, which is regulated by miR-20a-5p, miR-20b-5p, miR-92a-3p, and miR-17-5p, as shown in the ICN. Some of the ceRNA relationships that we predicted (Figure 4) have now been substantiated. A recent study conducted by Zhu et al.[35] proved one of the signaling pathways in the ICN. They found that the expression of *H19* was increased and miR-20b-5p was decreased in endometrial cancer tissues and cells. Additionally, *H19* accelerates the tumor formation of endometrial cancer through the miR-20b-5p/AXL/HIF-1α signaling pathway. Additionally, the knockdown of *H19* showed a therapeutic significance through the inhibition of tumor growth and the promotion of cell apoptosis. Moreover, we established a methotrexate resistance colon cancer cell line (HT29-MTX) to further prove the predicted signaling pathways in the ICN. Compared with HT29 cells, the *HIF1A* expression was upregulated in HT29-MTX cells (Figure S6A). This result was consistent with the findings that HIF-1α (encoded by *HIF1A*) confers drug resistance in colorectal cancer.[36] Simultaneously, we found that the expression of lncRNA *H19* was also upregulated in HT29-MTX cells (Figure S6B). The downregulation of *H19* upregulated miR-20a-5p, miR-20b-5p, and miR-17-5p in HT29-MTX cells (Figures S6C–S6F). Additionally, the relationship among *H19*/miR-17-5p/*HIF1A* has been validated (Figure S7). These results are also in accordance with the prediction in the ICN. Consistent with our findings, Huang et al.[37] found that *H19* was also upregulated in NSCLC cell lines. Silencing *H19* could suppress the growth, migration, and invasion of NSCLC cells via sponging miR-17. Similarly, Liu et al.[38] found that *H19* may competitively bind to miR-17a-5p and is thus involved in the pathogenesis of thyroid cancer. Additionally, Italiano et al.[39] identified that *THBS1* is the target of the miR17-92 cluster (miR-17, miR-18a, miR-19a, miR-20a, and miR-92a).

To further explore the role of ceRNA triplets in drug resistance, this study focused on genes in the ICN. We analyzed the correlation between drug sensitivities to 76 FDA-approved anti-cancer drugs and the transcriptional expressions of genes in the ICN. The genes in the ICN were potentially related to sensitivity and resistance of

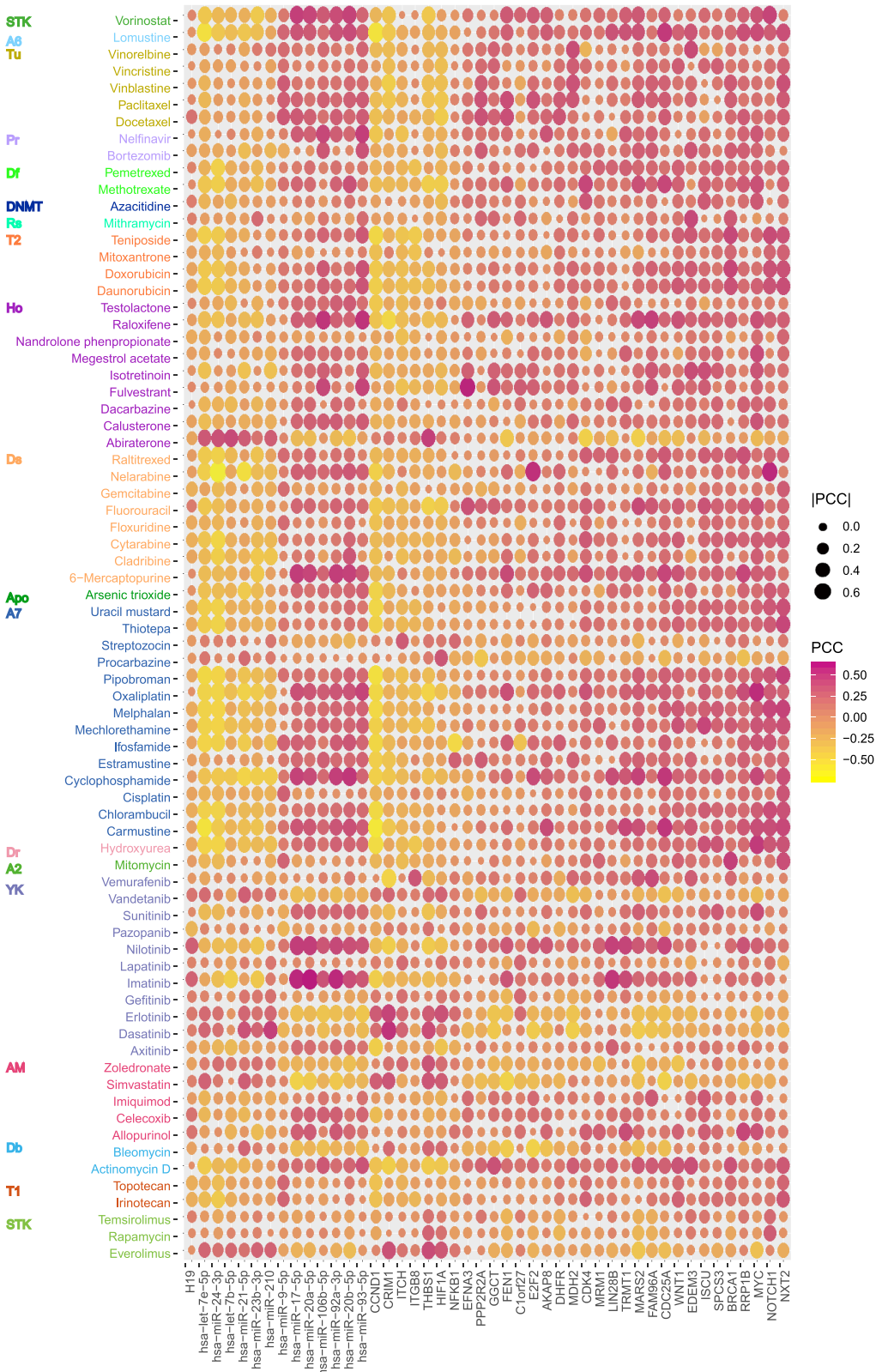

(legend on next page)

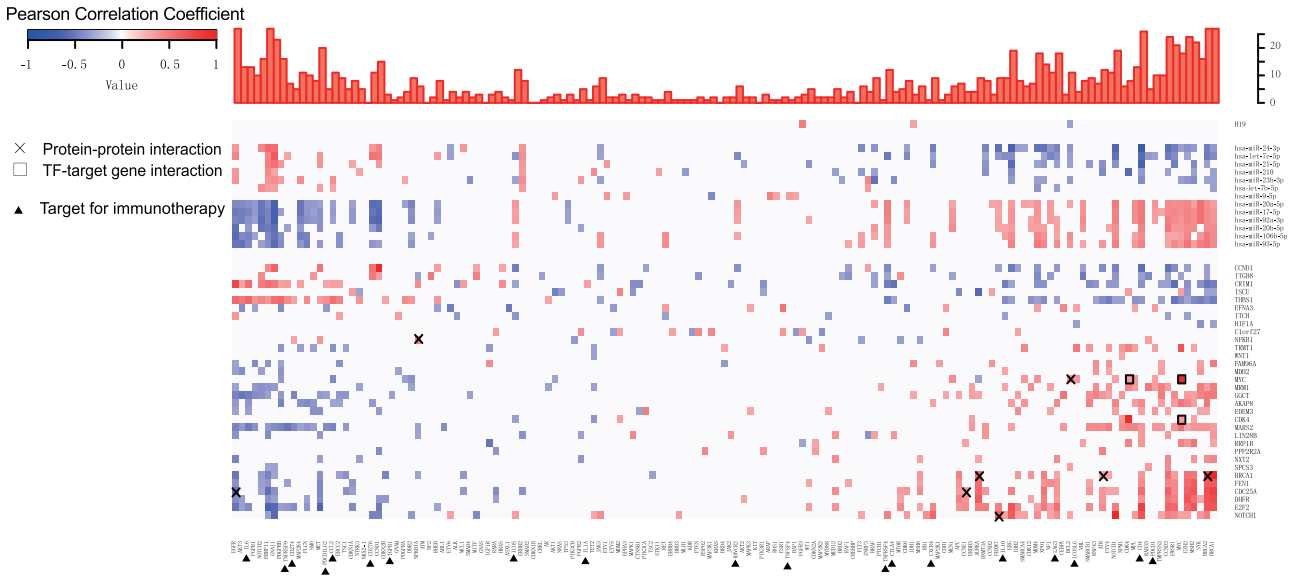

Figure 6. Correlation of transcriptional expression between genes in the ICN and clinically actionable genes (CAGs)

Pearson's correlation coefficients |R| > 0.3, p < 0.05; blue indicates a negative correlation; red indicates a positive correlation; color scale reflects Pearson's correlation coefficient. The x axis (CAGs) is ordered by the number of positively correlated genes in the ICN minus the number of negatively correlated genes in the ICN. The y axis (genes in the ICN) is ordered by the total number of correlated CAGs. If the number of cancer types is less than five, the fill color of the cell is white. Bold boxes highlight the transcriptional factor-gene interactions of CAGs and genes in the ICN. × marks the protein-protein interactions (PPIs) of CAGs and genes in the ICN based on the experimental evidence from HPRD.

various anti-cancer drugs (Figure 5). Some genes (e.g., *BRCA1*, *FAM96a*, *TRMT1*) are significantly correlated with resistance (positive correlation) to most anti-cancer drugs, while others (e.g., *ITCH*, miR-21-5p, miR-23b-3p) are genes in the ICN that are sensitive (negative correlation) to most anti-cancer drugs. These drug sensitivity- or resistance-correlated genes we identified are of clinical significance, and they may be novel predictors of drug sensitivity. Previous studies showed that *BRCA1*, miR-23b-3p, and *H19* were involved in the chemoresistance of cancer cells.[34,40,41] These findings were confirmed in our analysis. These results also indicate the genes that may potentially be involved in the sensitivity or resistance of anti-cancer drugs.

The genes in the ICN are likely to confer multi-drug resistance to cancers. To explore the clinical implications of the ICN, the interactions between genes in the ICN and CAGs were identified through co-expression, PPI, and transcription factor data (Figure 6). This result suggested that these genes in the ICN should be considered in cancer therapy. We observed some validated PPIs, including NOTCH1, CDC25A, BRCA1, MYC, and NFKB1. CDC5A was positively correlated to CCNE1 while negatively correlated to EGFR. These genes in the ICN could also act as transcriptional activators. For example, MYC could promote the transcription of *CDK4*.[42] Our results suggest that CAGs are regulated by the genes in the ICN, and they highlight the significance of these genes in the treatment of cancer.

Finally, we identified genes in the ICN that have potential clinical relevance based on the associations of the expression level with patient survival time and cancer stage (Figure 7A). Multiple genes are differentially expressed among tumor stages and associated with patient survival. For example, miR-20b-5p is positively correlated with the prognosis of patients in various cancers, including glioblastoma multiforme (GBM), HNSC, kidney renal papillary cell carcinoma (KIRP), liver hepatocellular carcinoma (LIHC), and PAAD. lncRNA *H19* is dysregulated in various cancers and correlated with the prognosis of patients (Figure 7A; Figure S9). Also, the expression level of *H19* in colon adenocarcinoma (COAD) depends on the individual cancer stage according to The Cancer Genome Atlas (TCGA) database (Figure S10). *E2F2* and *ITGB8* were negatively or positively correlated with the survival of cancer patients, respectively (Figure 7B). *E2F2* is a transcription factor that is upregulated in ovarian cancer. Enforced *E2F2* expression promotes *MCM4*, *CCNE2*, and *WHSC1* expression and is negatively correlated with the overall survival of ovarian cancer patients.[43] *ITGB8* encodes integrin beta 8, which is a transmembrane receptor. It is overexpressed in gefitinib-resistance HepG2 cells (HepG2/G). The silencing of *ITGB8* reversed

Figure 5. Correlation between drug sensitivity and genes in the ICN

Yellow indicates a negative correlation; red indicates a positive correlation; and size reflects absolute Pearson's correlation coefficient (p value). Color bars in the y axis indicate drugs and their category.

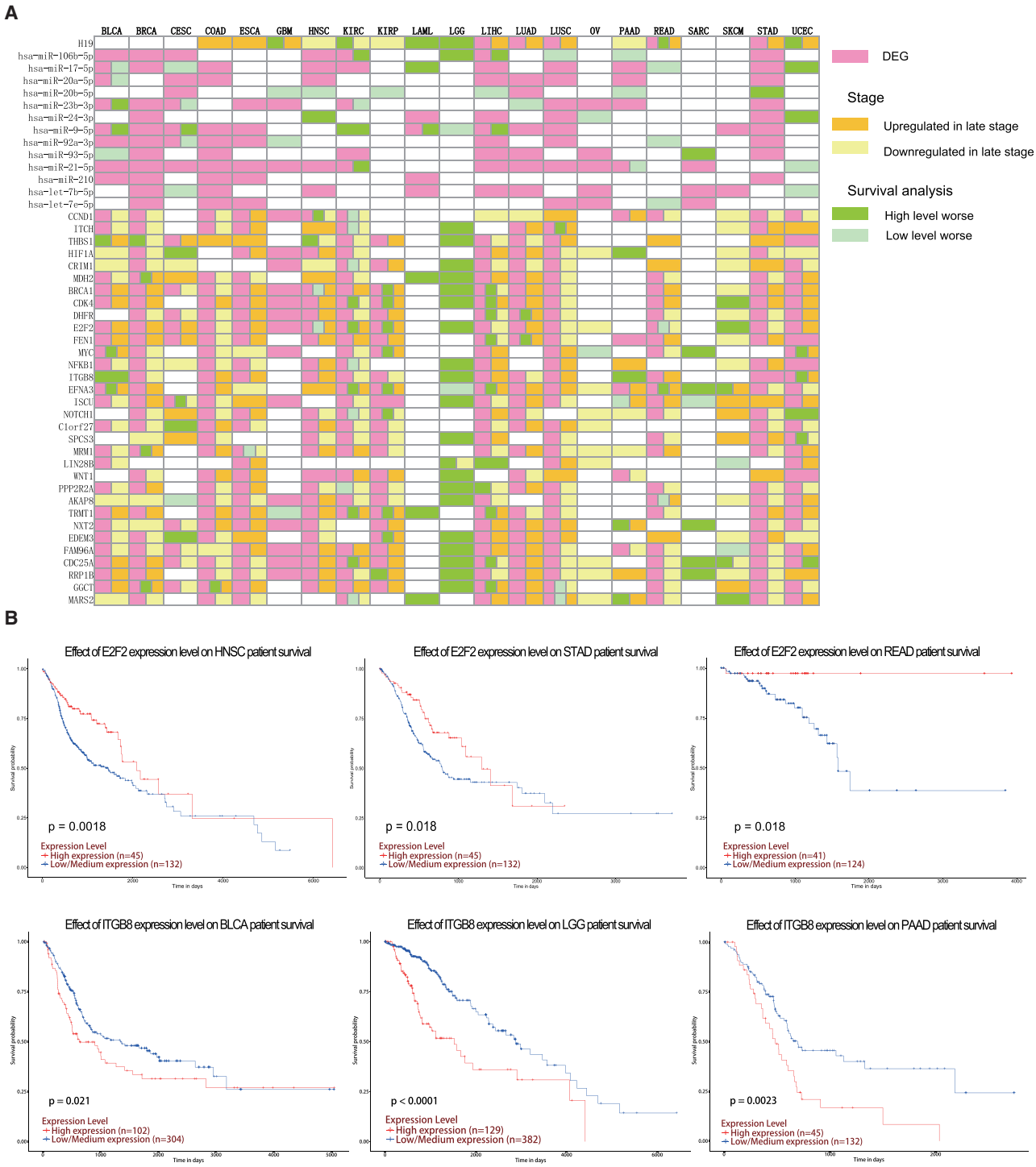

Figure 7. Clinical relevance of the ICN across 21 kinds of cancer.

(A) Clinical relevance of the ICN across different cancer types. Pink boxes indicate genes that are differently expressed between the ICN and different cancer samples. Dark yellow and light yellow boxes represent the upregulation or downregulation of genes in later stages (fold change of transcriptional expression between stages III/IV and stages I/II larger than 1.5). Dark green and light green boxes indicate high and low expression in tumors associated with worse overall survival times (log-rank test FDR < 0.05), respectively. (B) Kaplan-Meier curves of multiple cancer types stratified by median expression level of *E2F2* and *ITGB8*.

gefitinib resistance of HepG2 cells.[44] Similarly, the downregulation of *ITGB8* could also restore cisplatin resistance of ovarian cancer cells.[45] These results highlight the possible clinical utility of genes in the ICN in human cancer patients.

Our study provides a comprehensive analysis of the genes in the ICN across 15 drug categories and highlights their potential clinical utility in cancer therapy. The construction of the ICN suggested that a certain number of genes participate in multi-drug resistance. The design limitation in this work is that we only investigated single-drug effects, with no drug combination comparisons. In the following studies, we will assemble drug combination comparison data to strengthen our approach and predictability.

In summary, our study depicted the ceRNA crosstalk landscape across 15 anti-cancer drug categories. By systematically analyzing the ceRNA networks, we have revealed some important properties of ceRNA regulation. Additionally, our recent work characterized the small-molecule drugs and their affected lncRNAs.[46] These findings not only provide new insight into the investigation of anti-cancer drug resistance, but they also provide new insight into the clinical rational use of drugs.

MATERIALS AND METHODS

Candidate lncRNA-miRNA-PCG competing interactions

We obtained the lncRNA-miRNA-PCG interactions data using a previous study, which aimed to develop a pipeline to systematically identify lncRNA-associated competing triplets.[47] Briefly, the miRNA-lncRNA interactions were predicted using four miRNA target prediction methods, including miRanda (http://www.miranda.org/), RNAhybrid (https://bibiserv.cebitec.uni-bielefeld.de/rnahybrid/), TargetScan (http://www.targetscan.org/vert_72/), and PITA (https://genie.weizmann.ac.il/pubs/mir07/mir07_data.html). The miRNA-lncRNA interactions predicted based on different methods were integrated. Then, to identify experimentally supported miRNA-binding sites on lncRNA sequences, the Argonaute-cross-linking and immunoprecipitation (CLIP) data were used to filter the miRNA-lncRNA interactions. The miRNA-PCG interactions were obtained from two high-quality databases, TarBase (http://carolina.imis.athena-innovation.gr/diana_tools/web/index.php?r=tarbasev8%2Findex) and miRTarBase (http://mirtarbase.cuhk.edu.cn/php/index.php), that store manually curated collections of experimentally supported miRNA targets. lncRNA-PCG pairs that shared a single miRNA were regarded as one candidate lncRNA-miRNA-PCG competing interaction. Finally, we obtained 526173 non-redundant lncRNA-miRNA-PCG interactions for further analysis.

Generation of anti-cancer drug sensitivity-associated ceRNA networks

We collected drugs and drug-sensitivity-related PCGs and miRNAs from the CellMiner database (https://discover.nci.nih.gov/cellminer/).[48] The CellMiner database provides access to 60 human tumor cell lines (NCI-60 cell lines) and transcripts for 22,379 genes and 360 miRNAs along with activity reports for 20,503 chemical compounds including 102 drugs approved by the FDA.[48] In the CellMiner database, these anti-cancer drugs were divided into 15 drug categories according to their mode of action (Table S1). The transcripts were detected using untreated cell lines (NCI-60 cell lines), whereas the half-maximal inhibitory concentration (IC_{50}) was calculated after treatment of the cell lines. First, we selected FDA-approved drugs and clinical trial drugs and filtered out drugs not in the DrugBank (https://go.drugbank.com/) database. Then, we integrated all drug files downloaded from CellMiner, thus obtaining drug-miRNA and drug-PCG matrices.

lncRNA expression profiling in the NCI60 cancer cell line panel obtained by using high-throughput real-time PCR and corresponding data were downloaded from the GEO database (https://www.ncbi.nlm.nih.gov/geo/) (GEO: GSE80332). A drug-lncRNA matrix was constructed by calculating the PCC. Assigning 0.3 as the PCC threshold, we obtained 31,230 correlations of drug-lncRNA pairs, 9,557 of drug-miRNA pairs, and 363,654 of drug-PCG pairs.

Then, we performed some dealing steps to reduce false-positive results and construct the anti-cancer drug-sensitive ceRNA networks. For each drug, (1) we obtained the lncRNA-miRNA-PCG triplets that contain at least one drug-related gene ($|PCC| > 0.3$) and (2) the expressions of lncRNA and PCG should be positive or negative at the same time. Finally, we constructed 15 anti-cancer drug sensitivity-associated ceRNA networks (Table S1). The intersection edges of the 15 ceRNA networks were extracted and an ICN was constructed. The lncRNAs in the profiles of GEO: GSE80332 were selected for further analysis. In the ICN, most of the lncRNAs are not well characterized, and only *H19* was annotated. Therefore, *H19* was selected for the following analyses.

Collection of cancer-related lncRNAs, PCGs, and miRNAs

In order to explore the functional roles of these anti-cancer drug sensitivity-associated ceRNA networks in tumorigenesis, we examined whether lncRNAs, miRNAs and PCGs involved in them were intrinsic cancer driver genes or were closely associated with tumors. Thus, we collected the cancer-related lncRNA, PCG, and miRNA sets. The cancer-associated lncRNAs were downloaded from LncRNADisease (http://www.cuilab.cn/lncrnadisease).[49] In addition, cancer-related PCGs were extracted from COSMIC (https://www.sanger.ac.uk/cosmic)[50] and a previous study.[51] miRNAs associated with cancer were collected from miR2Disease (http://www.miR2Disease.org)[52] and HMDD (http://www.cuilab.cn/hmdd),[53] both of which are all manually curated databases for miRNA deregulation in human disease. In total, we obtained 20 lncRNAs, 324 PCGs, and 217 miRNAs that are associated with cancer. Then, a hypergeometric test was used to evaluate whether the genes in the anti-cancer drug sensitivity-associated ceRNA networks were significantly enriched in our collected cancer-related lncRNA, PCG, and miRNA sets.

Cancer hallmarks and functional analysis

Functional enrichment analysis was used to understand the functional roles of genes in the ceRNA networks. First, we derived the cancer

hallmark Gene Ontology (GO) terms from the research of Plaisier et al.[54] Then, the p values of the cumulative hypergeometric test were used to evaluate the significance of lncRNAs competitively regulating PCGs that enriched pathways/cancer hallmark GO terms. The cumulative hypergeometric test formula can be represented as follows:

$$P = 1 - \sum_{k=0}^{m} \frac{\binom{n}{k}\binom{N-n}{M-k}}{\binom{N}{M}}, \quad (1)$$

where N is all of the genome-wide genes, M is the number of a given GO term gene that is annotated in the N genes, n is the number of genes of a particular ceRNA, and m is the number of genes participating in a ceRNA network and annotated for the given cancer hallmark GO term.

Additionally, the Jaccard coefficient is used to calculate the similarity among 15 networks and is also used to measure intersections between cancer hallmark genes and PCGs in each ceRNA network. It is the ratio of intersection to union as follows:

$$\mathrm{Jac}(A,B) = \frac{|A \cap B|}{|A \cup B|} \mathrm{Jac}(A,B) = \frac{|A \cap B|}{|A \cup B|},$$

Interactions and correlations between genes in the ICN and CAGs

To derive a list of CAGs, we first obtained 132 target genes from Eliezer's study.[55] We also obtained 19 targeted genes for immunotherapy from another study.[56] We calculated PCC and considered |PCC| >0.3 with a p value <0.05 as a significant correlation between the transcriptional expressions of the genes in the ICN and CAGs. PPI data were obtained from HPRD (http://www.hprd.org/) and BioGRID (https://thebiogrid.org/), and transcription factor data were obtained from TRANSFAC (http://gene-regulation.com/pub/databases.html).[57]

Identification of clinically relevant genes in the ICN

To further identify genes in the intersection network that have potential clinical relevance based on the associations between the expression level, patient survival time, or cancer stage, the clinical data from TCGA database were collected.

The differential miRNAs between tumor and normal tissue were obtained from an online tool named miRNACancerMap (http://cis.hku.hk/miRNACancerMAP/).[58] Additionally, we downloaded TCGA survival data and molecular subtypes of cancer from OncoLnc (http://www.oncolnc.org/) and UALCAN (http://ualcan.path.uab.edu/index.html).[59]

These tools performed a log-rank test to calculate the association between the expression of genes in the ICN and overall survival. Transcript expression levels were categorized by the upper quartile of transcripts per kilobase of exon model per million mapped reads (TPM), and a p value <0.05 was considered to denote statistical significance. UALCAN used a t test to detect genes in the ICN with differential expressions among different disease stages, and we considered a p value < 0.05 to denote a significant difference.

SUPPLEMENTAL INFORMATION

Supplemental information can be found online at https://doi.org/10.1016/j.omtn.2021.02.011.

ACKNOWLEDGMENTS

This work was supported by the National Natural Science Foundation of China (81803524 and 81803012); the China Postdoctoral Science Foundation (2018M641878); the HeiLongJiang Postdoctoral Foundation (LBH-Q19161 and LBH-Z18168); the Foundation of Health and Family Planning Commission of Heilongjiang Province (2018465 and 2018484).

AUTHOR CONTRIBUTIONS

D.S., Z.Q., and Y.J. designed the study. B.L., X. Zhou, D.W., and X. Zhang collected data. D.S., X. Zhou, and X.S. developed the computational model and analyzed the network. D.S., Y.J., and B.L. wrote the article. Z.Q. performed the cell culture and real-time PCR analysis. All authors reviewed the manuscript.

DECLARATION OF INTERESTS

The authors declare no competing interests.

REFERENCES

1. World Health Organization (2018). Cancer, https://www.who.int/news-room/fact-sheets/detail/cancer.
2. Bray, F., Ferlay, J., Soerjomataram, I., Siegel, R.L., Torre, L.A., and Jemal, A. (2018). Global cancer statistics 2018: GLOBOCAN estimates of incidence and mortality worldwide for 36 cancers in 185 countries. CA Cancer J. Clin. *68*, 394–424.
3. Brown, R., Curry, E., Magnani, L., Wilhelm-Benartzi, C.S., and Borley, J. (2014). Poised epigenetic states and acquired drug resistance in cancer. Nat. Rev. Cancer *14*, 747–753.
4. Kage, K., Tsukahara, S., Sugiyama, T., Asada, S., Ishikawa, E., Tsuruo, T., and Sugimoto, Y. (2002). Dominant-negative inhibition of breast cancer resistance protein as drug efflux pump through the inhibition of S-S dependent homodimerization. Int. J. Cancer *97*, 626–630.
5. He, Z., Xiao, X., Li, S., Guo, Y., Huang, Q., Shi, X., Wang, X., and Liu, Y. (2017). Oridonin induces apoptosis and reverses drug resistance in cisplatin resistant human gastric cancer cells. Oncol. Lett. *14*, 2499–2504.
6. Lee, Y.S., Kim, S.M., Kim, B.W., Chang, H.J., Kim, S.Y., Park, C.S., Park, K.C., and Chang, H.S. (2018). Anti-cancer effects of HNHA and lenvatinib by the suppression of EMT-mediated drug resistance in cancer stem cells. Neoplasia *20*, 197–206.
7. Schmitt, A., Knittel, G., Welcker, D., Yang, T.P., George, J., Nowak, M., Leeser, U., Büttner, R., Perner, S., Peifer, M., and Reinhardt, H.C. (2017). *ATM* deficiency is associated with sensitivity to PARP1- and ATR inhibitors in lung adenocarcinoma. Cancer Res. *77*, 3040–3056.
8. Miao, Y., Zheng, W., Li, N., Su, Z., Zhao, L., Zhou, H., and Jia, L. (2017). MicroRNA-130b targets PTEN to mediate drug resistance and proliferation of breast cancer cells via the PI3K/Akt signaling pathway. Sci. Rep. *7*, 41942.
9. Wu, H., Zhou, J., Mei, S., Wu, D., Mu, Z., Chen, B., Xie, Y., Ye, Y., and Liu, J. (2017). Circulating exosomal microRNA-96 promotes cell proliferation, migration and drug resistance by targeting LMO7. J. Cell. Mol. Med. *21*, 1228–1236.

10. Malek, E., Jagannathan, S., and Driscoll, J.J. (2014). Correlation of long non-coding RNA expression with metastasis, drug resistance and clinical outcome in cancer. Oncotarget *5*, 8027–8038.

11. Liu, X.H., Liu, Z.L., Sun, M., Liu, J., Wang, Z.X., and De, W. (2013). The long non-coding RNA HOTAIR indicates a poor prognosis and promotes metastasis in non-small cell lung cancer. BMC Cancer *13*, 464.

12. Sørensen, K.P., Thomassen, M., Tan, Q., Bak, M., Cold, S., Burton, M., Larsen, M.J., and Kruse, T.A. (2013). Long non-coding RNA HOTAIR is an independent prognostic marker of metastasis in estrogen receptor-positive primary breast cancer. Breast Cancer Res. Treat. *142*, 529–536.

13. Kim, K., Jutooru, I., Chadalapaka, G., Johnson, G., Frank, J., Burghardt, R., Kim, S., and Safe, S. (2013). HOTAIR is a negative prognostic factor and exhibits pro-oncogenic activity in pancreatic cancer. Oncogene *32*, 1616–1625.

14. Liu, Z., Sun, M., Lu, K., Liu, J., Zhang, M., Wu, W., De, W., Wang, Z., and Wang, R. (2013). The long noncoding RNA HOTAIR contributes to cisplatin resistance of human lung adenocarcinoma cells via downregualtion of $p21^{WAF1/CIP1}$ expression. PLoS ONE *8*, e77293.

15. Shi, S.J., Wang, L.J., Yu, B., Li, Y.H., Jin, Y., and Bai, X.Z. (2015). lncRNA-ATB promotes trastuzumab resistance and invasion-metastasis cascade in breast cancer. Oncotarget *6*, 11652–11663.

16. Tsang, W.P., Wong, T.W., Cheung, A.H., Co, C.N., and Kwok, T.T. (2007). Induction of drug resistance and transformation in human cancer cells by the noncoding RNA CUDR. RNA *13*, 890–898.

17. Salmena, L., Poliseno, L., Tay, Y., Kats, L., and Pandolfi, P.P. (2011). A ceRNA hypothesis: the Rosetta Stone of a hidden RNA language? Cell *146*, 353–358.

18. Qu, L., Ding, J., Chen, C., Wu, Z.J., Liu, B., Gao, Y., Chen, W., Liu, F., Sun, W., Li, X.F., et al. (2016). Exosome-transmitted lncARSR promotes sunitinib resistance in renal cancer by acting as a competing endogenous RNA. Cancer Cell *29*, 653–668.

19. Li, Y., Ye, Y., Feng, B., and Qi, Y. (2017). Long noncoding RNA lncARSR promotes doxorubicin resistance in hepatocellular carcinoma via modulating PTEN-PI3K/Akt pathway. J. Cell. Biochem. *118*, 4498–4507.

20. Gu, J., Wang, Y., Wang, X., Zhou, D., Shao, C., Zhou, M., and He, Z. (2018). Downregulation of lncRNA GAS5 confers tamoxifen resistance by activating miR-222 in breast cancer. Cancer Lett. *434*, 1–10.

21. Yildirim, M.A., Goh, K.I., Cusick, M.E., Barabási, A.L., and Vidal, M. (2007). Drug-target network. Nat. Biotechnol. *25*, 1119–1126.

22. Han, J.D., Bertin, N., Hao, T., Goldberg, D.S., Berriz, G.F., Zhang, L.V., Dupuy, D., Walhout, A.J., Cusick, M.E., Roth, F.P., and Vidal, M. (2004). Evidence for dynamically organized modularity in the yeast protein-protein interaction network. Nature *430*, 88–93.

23. Jin, G., Zhang, S., Zhang, X.S., and Chen, L. (2007). Hubs with network motifs organize modularity dynamically in the protein-protein interaction network of yeast. PLoS ONE *2*, e1207.

24. Ekman, D., Light, S., Björklund, A.K., and Elofsson, A. (2006). What properties characterize the hub proteins of the protein-protein interaction network of *Saccharomyces cerevisiae*? Genome Biol. *7*, R45.

25. Imig, J., Brunschweiger, A., Brümmer, A., Guennewig, B., Mittal, N., Kishore, S., Tsikrika, P., Gerber, A.P., Zavolan, M., and Hall, J. (2015). miR-CLIP capture of a miRNA targetome uncovers a lincRNA H19-miR-106a interaction. Nat. Chem. Biol. *11*, 107–114.

26. Fu, Z., Li, G., Li, Z., Wang, Y., Zhao, Y., Zheng, S., Ye, H., Luo, Y., Zhao, X., Wei, L., et al. (2017). Endogenous miRNA sponge lincRNA-ROR promotes proliferation, invasion and stem cell-like phenotype of pancreatic cancer cells. Cell Death Discov. *3*, 17004.

27. Wang, E., Zaman, N., Mcgee, S., Milanese, J.S., Masoudi-Nejad, A., and O'Connor-McCourt, M. (2015). Predictive genomics: a cancer hallmark network framework for predicting tumor clinical phenotypes using genome sequencing data. Semin. Cancer Biol. *30*, 4–12.

28. Peri, S., Navarro, J.D., Kristiansen, T.Z., Amanchy, R., Surendranath, V., Muthusamy, B., Gandhi, T.K., Chandrika, K.N., Deshpande, N., Suresh, S., et al. (2004). Human protein reference database as a discovery resource for proteomics. Nucleic Acids Res. *32*, D497–D501.

29. Chatr-Aryamontri, A., Breitkreutz, B.J., Oughtred, R., Boucher, L., Heinicke, S., Chen, D., Stark, C., Breitkreutz, A., Kolas, N., O'Donnell, L., et al. (2015). The BioGRID interaction database: 2015 update. Nucleic Acids Res. *43*, D470–D478.

30. Liu, H., Wang, S., Zhou, S., Meng, Q., Ma, X., Song, X., Wang, L., and Jiang, W. (2019). Drug resistance-related competing interactions of lncRNA and mRNA across 19 cancer types. Mol. Ther. Nucleic Acids *16*, 442–451.

31. Kesarwani, M., Kincaid, Z., Gomaa, A., Huber, E., Rohrabaugh, S., Siddiqui, Z., Bouso, M.F., Latif, T., Xu, M., Komurov, K., et al. (2017). Targeting c-FOS and DUSP1 abrogates intrinsic resistance to tyrosine-kinase inhibitor therapy in BCR-ABL-induced leukemia. Nat. Med. *23*, 472–482.

32. Zhu, J., Zhang, R., Yang, D., Li, J., Yan, X., Jin, K., Li, W., Liu, X., Zhao, J., Shang, W., and Yu, T. (2018). Knockdown of long non-coding RNA XIST inhibited doxorubicin resistance in colorectal cancer by upregulation of miR-124 and downregulation of SGK1. Cell. Physiol. Biochem *51*, 113–128.

33. Jiang, P., Chen, A., Wu, X., Zhou, M., Ul Haq, I., Mariyam, Z., and Feng, Q. (2018). NEAT1 acts as an inducer of cancer stem cell-like phenotypes in NSCLC by inhibiting EGCG-upregulated CTR1. J. Cell. Physiol. *233*, 4852–4863.

34. Zheng, Z.G., Xu, H., Suo, S.S., Xu, X.L., Ni, M.W., Gu, L.H., Chen, W., Wang, L.Y., Zhao, Y., Tian, B., and Hua, Y.J. (2016). The essential role of H19 contributing to cisplatin resistance by regulating glutathione metabolism in high-grade serous ovarian cancer. Sci. Rep. *6*, 26093.

35. Zhu, H., Jin, Y.M., Lyu, X.M., Fan, L.M., and Wu, F. (2019). Long noncoding RNA H19 regulates HIF-1α/AXL signaling through inhibiting miR-20b-5p in endometrial cancer. Cell Cycle *18*, 2454–2464.

36. Wang, Y., Lei, F., Rong, W., Zeng, Q., and Sun, W. (2015). Positive feedback between oncogenic KRAS and HIF-1α confers drug resistance in colorectal cancer. OncoTargets Ther. *8*, 1229–1237.

37. Huang, Z., Lei, W., Hu, H.B., Zhang, H., and Zhu, Y. (2018). H19 promotes non-small-cell lung cancer (NSCLC) development through STAT3 signaling via sponging miR-17. J. Cell. Physiol. *233*, 6768–6776.

38. Liu, L., Yang, J., Zhu, X., Li, D., Lv, Z., and Zhang, X. (2016). Long noncoding RNA H19 competitively binds miR-17-5p to regulate YES1 expression in thyroid cancer. FEBS J. *283*, 2326–2339.

39. Italiano, A., Thomas, R., Breen, M., Zhang, L., Crago, A.M., Singer, S., Khanin, R., Maki, R.G., Mihailovic, A., Hafner, M., et al. (2012). The miR-17-92 cluster and its target *THBS1* are differentially expressed in angiosarcomas dependent on *MYC* amplification. Genes Chromosomes Cancer *51*, 569–578.

40. Tassone, P., Tagliaferri, P., Perricelli, A., Blotta, S., Quaresima, B., Martelli, M.L., Goel, A., Barbieri, V., Costanzo, F., Boland, C.R., and Venuta, S. (2003). BRCA1 expression modulates chemosensitivity of BRCA1-defective HCC1937 human breast cancer cells. Br. J. Cancer *88*, 1285–1291.

41. An, Y., Zhang, Z., Shang, Y., Jiang, X., Dong, J., Yu, P., Nie, Y., and Zhao, Q. (2015). miR-23b-3p regulates the chemoresistance of gastric cancer cells by targeting ATG12 and HMGB2. Cell Death Dis. *6*, e1766.

42. Hermeking, H., Rago, C., Schuhmacher, M., Li, Q., Barrett, J.F., Obaya, A.J., O'Connell, B.C., Mateyak, M.K., Tam, W., Kohlhuber, F., et al. (2000). Identification of *CDK4* as a target of c-MYC. Proc. Natl. Acad. Sci. USA *97*, 2229–2234.

43. Xie, L., Li, T., and Yang, L.H. (2017). E2F2 induces MCM4, CCNE2 and WHSC1 up-regulation in ovarian cancer and predicts poor overall survival. Eur. Rev. Med. Pharmacol. Sci. *21*, 2150–2156.

44. Wang, W.W., Wang, Y.B., Wang, D.Q., Lin, Z., and Sun, R.J. (2015). Integrin beta-8 (ITGB8) silencing reverses gefitinib resistance of human hepatic cancer HepG2/G cell line. Int. J. Clin. Exp. Med. *8*, 3063–3071.

45. Cui, Y., Wu, F., Tian, D., Wang, T., Lu, T., Huang, X., Zhang, P., and Qin, L. (2018). miR-199a-3p enhances cisplatin sensitivity of ovarian cancer cells by targeting ITGB8. Oncol. Rep. *39*, 1649–1657.

46. Yang, H., Jiang, Y., Zhang, Y., Xu, Y., Zhang, C., Han, J., Su, F., Liu, X., Mi, K., Liu, B., and Shang, D. (2019). System level characterization of small molecule drugs and their affected long noncoding RNAs. Aging (Albany NY) *11*, 12428–12451.

47. Wang, P., Ning, S., Zhang, Y., Li, R., Ye, J., Zhao, Z., Zhi, H., Wang, T., Guo, Z., and Li, X. (2015). Identification of lncRNA-associated competing triplets reveals global patterns and prognostic markers for cancer. Nucleic Acids Res. *43*, 3478–3489.

48. Reinhold, W.C., Sunshine, M., Liu, H., Varma, S., Kohn, K.W., Morris, J., Doroshow, J., and Pommier, Y. (2012). CellMiner: a web-based suite of genomic and pharmacologic tools to explore transcript and drug patterns in the NCI-60 cell line set. Cancer Res. *72*, 3499–3511.

49. Chen, G., Wang, Z., Wang, D., Qiu, C., Liu, M., Chen, X., Zhang, Q., Yan, G., and Cui, Q. (2013). LncRNADisease: a database for long-non-coding RNA-associated diseases. Nucleic Acids Res. *41*, D983–D986.

50. Forbes, S.A., Bindal, N., Bamford, S., Cole, C., Kok, C.Y., Beare, D., Jia, M., Shepherd, R., Leung, K., Menzies, A., et al. (2011). COSMIC: mining complete cancer genomes in the Catalogue of Somatic Mutations in Cancer. Nucleic Acids Res. *39*, D945–D950.

51. Tamborero, D., Gonzalez-Perez, A., Perez-Llamas, C., Deu-Pons, J., Kandoth, C., Reimand, J., Lawrence, M.S., Getz, G., Bader, G.D., Ding, L., and Lopez-Bigas, N. (2013). Comprehensive identification of mutational cancer driver genes across 12 tumor types. Sci. Rep. *3*, 2650.

52. Jiang, Q., Wang, Y., Hao, Y., Juan, L., Teng, M., Zhang, X., Li, M., Wang, G., and Liu, Y. (2009). miR2Disease: a manually curated database for microRNA deregulation in human disease. Nucleic Acids Res. *37*, D98–D104.

53. Li, Y., Qiu, C., Tu, J., Geng, B., Yang, J., Jiang, T., and Cui, Q. (2014). HMDD v2.0: a database for experimentally supported human microRNA and disease associations. Nucleic Acids Res. *42*, D1070–D1074.

54. Plaisier, C.L., Pan, M., and Baliga, N.S. (2012). A miRNA-regulatory network explains how dysregulated miRNAs perturb oncogenic processes across diverse cancers. Genome Res. *22*, 2302–2314.

55. Van Allen, E.M., Wagle, N., Stojanov, P., Perrin, D.L., Cibulskis, K., Marlow, S., Jane-Valbuena, J., Friedrich, D.C., Kryukov, G., Carter, S.L., et al. (2014). Whole-exome sequencing and clinical interpretation of formalin-fixed, paraffin-embedded tumor samples to guide precision cancer medicine. Nat. Med. *20*, 682–688.

56. Mak, M.P., Tong, P., Diao, L., Cardnell, R.J., Gibbons, D.L., William, W.N., Skoulidis, F., Parra, E.R., Rodriguez-Canales, J., Wistuba, I.I., et al. (2016). A patient-derived, pan-cancer EMT signature identifies global molecular alterations and immune target enrichment following epithelial-to-mesenchymal transition. Clin. Cancer Res *22*, 609–620.

57. Wingender, E., Chen, X., Hehl, R., Karas, H., Liebich, I., Matys, V., Meinhardt, T., Prüss, M., Reuter, I., and Schacherer, F. (2000). TRANSFAC: an integrated system for gene expression regulation. Nucleic Acids Res. *28*, 316–319.

58. Tong, Y., Ru, B., and Zhang, J. (2018). miRNACancerMAP: an integrative web server inferring miRNA regulation network for cancer. Bioinformatics *34*, 3211–3213.

59. Chandrashekar, D.S., Bashel, B., Balasubramanya, S.A.H., Creighton, C.J., Ponce-Rodriguez, I., Chakravarthi, B.V.S.K., and Varambally, S. (2017). UALCAN: a portal for facilitating tumor subgroup gene expression and survival analyses. Neoplasia *19*, 649–658.